Correlation of native defects between epitaxial films and polycrystalline $BaSi_2$ bulks based on photoluminescence spectra

Takuma Sato[1,2], Yudai Yamashita[1], Zhihao Xu[1], Kaoru Toko[1], Serge Gambarelli[2], Motoharu Imai[3], and Takashi Suemasu[1]

[1]*Institute of Applied Physics, University of Tsukuba, Tsukuba, Ibaraki 305-8573, Japan*

[2]*Université Grenoble Alpes, CEA, CNRS, IRIG, SyMMES, 38000 Grenoble, France*

[3]*Research Center for Functional Materials, National Institute for Materials Science, Ibaraki 305-0047, Japan*

We conducted photoluminescence (PL) measurements at 8 K on $BaSi_2$ epitaxial films and polycrystalline bulks. PL intensities were enhanced for films grown at 650 °C compared to those at 580 °C due to reduction of carrier recombination centers. PL spectra were fitted well by four Gaussian curves peaking at almost the same energies regardless of film and bulk forms. Their contribution changed depending on Ba-to-Si atomic ratios in $BaSi_2$. Based on the PL spectra and defect levels acquired by deep level transient spectroscopy, we established a model for radiative defects which stem from intrinsic defects such as Si vacancies.

* Corresponding author at:
Institute of Applied Physics, Faculty of Pure and Applied Sciences, University of Tsukuba, Tsukuba, Ibaraki 305-8573, Japan
Electronic mail: suemasu@bk.tsukuba.ac.jp

We have paid special attention to barium disilicide ($BaSi_2$) consisting of less-toxic and earth-abundant elements.[1,2] This environmentally friendly material shows a high optical absorption coefficient $\alpha = 3 \times 10^4\ cm^{-1}$ at 1.5 eV (more than 40 times as large as that of crystalline Si) in spite of an indirect bandgap semiconductor (E_g = 1.3 eV at room temperature).[3-5] In addition, it possesses superior minority carrier properties.[6-10] Thus, we consider $BaSi_2$ as one of the most promising candidates for a single-junction solar cell. We recently have demonstrated the operation of homojunction solar cells.[11] We are now focusing on further improvement of $BaSi_2$ light absorbing layers with less defects. Because of limited studies on defects in $BaSi_2$,[12-15] many questions concerning fundamental defect information of $BaSi_2$ films and bulks have yet to be answered. The understanding and controlling of such defects is one of the indispensable prerequisites that have to be met in order to realize less defective layers. According to Kumar *et al*., Si vacancies (V_{Si}) are most likely to exist as intrinsic defects in $BaSi_2$, which induce defect levels within the bandgap.[16] This is the reason why Ba-to-Si deposition rate ratios (R_{Ba}/R_{Si}) during molecular beam epitaxy (MBE) significantly affect optical and electrical properties of the films.[17] Therefore, as a first step, the information of intrinsic defects caused by deviations from stoichiometry have to be investigated. Photoluminescence (PL) offers a nondestructive and sensitive tool for defect studies in solar cell materials such as Si.[18-20] However, PL reports dealing with single crystalline $BaSi_2$[21] and epitaxial layers[15,22] have been quite limited. In our previous research,[15] PL intensities decreased when the R_{Ba}/R_{Si} approached the stoichiometry. Due to their weak PL intensities, however, it was hard to examine the relationship between the PL intensities and defects and further refer to origins of such radiative defects. Recently, we found that the PL intensity was enhanced significantly in $BaSi_2$ films grown at higher temperatures (T_S) during the MBE growth.[14] In this letter, we performed PL measurements of *a*-axis-oriented $BaSi_2$ epitaxial films with different values of R_{Ba}/R_{Si} and polycrystalline $BaSi_2$ bulks formed from different Ba-to-Si starting material ratios, and

compared their spectra. Such $BaSi_2$ epitaxial films contain three epitaxial variants rotating around the surface normal by 120°.[6,23] Grain boundaries between epitaxial variants in *a*-axis-oriented $BaSi_2$ epitaxial films do not act as electrically active defects from the viewpoints of first-principle calculation[24] and experiment.[10] We found that the PL spectra were reproduced well by four Gaussian curves in both cases. We discuss the origin of these PL peaks and propose a model explaining radiative defects of $BaSi_2$.

We used an MBE system equipped with an electron-beam evaporation source for 10N-Si and standard Knudsen cells for 3N-Ba. First, we grew 0.5 μm-thick *a*-axis-oriented $BaSi_2$ epitaxial layers by MBE on Czochralski (CZ) n^+-Si(111) substrates (resistivity $\rho < 0.01$ Ωcm) at 580 and 650 °C. Details of the growth procedure of $BaSi_2$ films were reported previously.[14,17] In order to investigate the effect of variation of R_{Ba}/R_{Si} during the MBE growth on PL, we fixed R_{Si} to 0.9 nm/min and varied R_{Ba} from 0.8 to 3.3 nm/min, giving a variation of R_{Ba}/R_{Si} from 0.9 to 3.7. Sample preparation details were shown in Table I. The optimum R_{Ba}/R_{Si} was found to be 2.2 and 1.2, respectively, at T_S = 580 and 650 °C from the viewpoint of photoresponsivity (PR).[14,17] Epitaxial growth of *a*-axis-oriented $BaSi_2$ was confirmed from the θ–2θ x-ray diffraction (XRD; Rigaku Smart Lab) and reflection high-energy electron diffraction patterns. The polycrystalline bulk samples were prepared by Ar-arc melting of x_s : 1 (x_s = 0.515, 0.500, 0.485, and 0.476) molar mixture of Ba (nominal purity 3N) and Si (nominal purity 10N). The chemical compositions of synthesized polycrystalline bulk samples were determined by inductively coupled-plasma optical emission spectroscopy (ICP-OES). Table II lists the Ba-to-Si ratio of the starting materials x_s and that of synthesized samples (N_{Ba}/N_{Si}). As a measured of the optical properties of the films, PR spectra were measured at room temperature by using a lock-in technique with a xenon lamp and a 25-cm-focal-length single monochromator (Bunko Keiki SM-1700A and RU-60N). We applied a bias voltage (V_{bias}) to the front indium-tin-oxide (ITO) electrode with respect to the backside Al electrode. PL measurements were carried out at

8–80 K with the excitation laser light of 442 nm and detected by a liquid nitrogen cooled InP/InGaAs photomultiplier (Hamamatsu Photonics R5509-72) and amplified by the lock-in technique. Samples were excited from the $BaSi_2$ side.

Table I. Film sample preparation details. Si substrate, $BaSi_2$ layer thicknesses, R_{Ba}/R_{Si}, and Si substrate temperature (T_S) during MBE growth are given.

Sample	Si substrate	$BaSi_2$ layer	R_{Ba}/R_{Si}	T_S [°C]
A	CZ n^+-Si(111), $\rho < 0.01$ Ωcm	0.5 μm	2.2	580
B	CZ n^+-Si(111), $\rho < 0.01$ Ωcm	0.5 μm	1.2	650
C	CZ n^+-Si(111), $\rho < 0.01$ Ωcm	0.5 μm	0.9	650
D	CZ n^+-Si(111), $\rho < 0.01$ Ωcm	0.5 μm	1.5	650
E	CZ n^+-Si(111), $\rho < 0.01$ Ωcm	0.5 μm	2.3	650
F	CZ n^+-Si(111), $\rho < 0.01$ Ωcm	0.5 μm	3.7	650

Figure 1(a) showed PL spectra of samples A and B. The only difference between them is the growth temperature during the MBE growth. Sample B, grown at higher temperature, shows more intense PL than sample A, while sample B shows more intense PR as seen in Fig. 1(b). In PL measurements, only radiative recombination processes are possible to be observed. On the other hand, in PR measurements, photogenerated carriers reaching the electrodes before recombination via defect levels are detected. Therefore, this result indicates that nonradiative

and/or undetectable defects which are impossible to be detected in PL were smaller in sample B than in sample A. According to first-principle calculations in our previous work,[13] a Raman peak originating from V_{Si} appears at around 480 cm^{-1}. Because of overlapping with the most intense Raman peak due to A_g mode in $BaSi_2$, we cannot decompose each spectrum at room temperature, yet we confirmed that the full-width at half maximum (FWHM) including a contribution of V_{Si} decreased by approximately 7% in the film grown at T_S = 650 °C compared with sample A grown at T_S = 580 °C as shown in Fig. 1(c). As discussed in Ref. [14], the decrease of FWHM is correlated with the decrease of V_{Si}. Thus, we ascribe the enhancement of PL intensity in sample B to the decrease of nonradiative (or undetectable) recombination centers. The enhancement of PL intensity enables us to investigate radiative defects in the films grown with a wide range of R_{Ba}/R_{Si}.

Figures 2(a)-(d) show temperature dependencies of PL spectra of samples C-F grown at T_S = 650 °C. Although the variation of R_{Ba}/R_{Si} made their PL spectra look differently, we observed four different transitions marked as P1, P2, P3, and P4 in all samples. An example of the fitting result is shown in Fig. 2(e). The observed PL peaks (P1–4) are located at around 0.83, 0.95, 1.03, and 1.12 eV, respectively. In order to verify all the observed PL peaks originating from the bulk region of the films (neither from the interface between the $BaSi_2$ films and the Si substrate nor from the bulk region of the substrate), we also performed PL measurements on polycrystalline bulk samples. The PL spectra drastically changed from sample to sample depending on N_{Ba}/N_{Si} as shown in Fig. 3(a). Interestingly, we also observed four PL peaks at almost the same energies as those observed in the films with much better signal to noise (S/N) ratios.

Table II. Ratio of Ba to Si in the starting materials x_s and that in the synthesized polycrystalline bulk samples N_{Ba}/N_{Si}. N_{Ba}/N_{Si} was determined by ICP-OES.

Sample	Starting materials, x_s	Synthesized materials, N_{Ba}/N_{Si}
G	0.515	0.513
H	0.500	0.495
I	0.485	0.478
J	0.476	0.415

For further understandings on these PL transitions, we next performed the excitation intensity (P_{exc}) dependence of PL intensity. We chose sample I for this measurement because it showed the highest S/N ratio and possessed distinct P1–4 PL transitions among all the samples. In the typical cases of defect-correlated recombination mechanism, the PL intensity I_{PL} shows a power law followed by $I_{PL} \propto P_{exc}{}^{k}$ with an exponent $k < 1$.[25,26] All transitions followed the power law with $k = 0.52 - 0.66$ as shown in Fig. 3(b). Thus, we assigned all the observed PL peaks to donor-to-acceptor transitions. An observation of band-to-band or band-to-donor (acceptor) transitions can be very informative for us to assign PL spectra to the corresponding defect levels. In the present study, however, we did not observed such transitions ($k > 1$).

Based on the obtained results, we next discuss origins of each PL peak. Experimentally obtained defect levels are summarized in Table III.

Table III. Reported defect levels.

Defect level	Shape of sample	Measured by	Reference
$E_C - E_t = 0.26$ eV	Polycrystalline bulk	resistivity	27
$E_C - E_t = 0.13$ eV	Polycrystalline bulk	resistivity	27
$E_t - E_V = 0.27$ eV	Epitaxial film	DLTS	12

According to first-principle calculations,[16] V_{Si}, self-interstitial Si (Si_i), and Ba antisite for Si (Ba_{Si}) are considered as intrinsic defects in $BaSi_2$. Such defects are formed with different concentrations under Si-rich and Ba-rich conditions. We compared relative PL intensity of each peak among the films and polycrystalline bulks in Fig. 4. In the polycrystalline bulks, the ratio of P1 intensity decreased with increasing N_{Ba}/N_{Si} while those of P3 and P4 increased in Fig. 4(b). In contrast, the PL spectra of the films show a little complexity in Fig. 4(a). One of the factors which make the R_{Ba}/R_{Si} dependence of P1–4 intensity ratio complicated for the films is the diffusion of Si atoms from the Si substrate into grown layers. It was found from Rutherford backscattering spectroscopy that the Ba/Si atomic ratio in a $BaSi_2$ film decreased when it approached the $BaSi_2$/Si interface for all the samples even though they were grown under a constant value of R_{Ba}/R_{Si} during the growth.[17] Besides we recently found that excess Si atoms in $BaSi_2$ films grown under Si rich conditions diffused out from the $BaSi_2$ layers and precipitated around the $BaSi_2$/Si interface, leading to the degradation of *a*-axis orientation of $BaSi_2$ and quite rough $BaSi_2$/Si interfaces. Judging from these situations, we focus on the results of polycrystalline bulks in this article, where we can neglect such atomic distributions. Because Kumar *et al*. pointed out that V_{Si} are dominant point defects in $BaSi_2$ even under Si-rich conditions,[16] we suppose the most distinct PL peak, P1, is related to V_{Si}. On the other hand, P1 became most intense in sample J grown under Si-rich conditions. Hence, it is reasonable to assign Si_i as its counterpart. In the vicinity of stoichiometry, the intensity of P1 decreased because of the decrease in the amount of V_{Si} and/or Si_i defects. In $BaSi_2$ epitaxial films passivated with atomic H, which might be consider to fill V_{Si}, the intensity of P1 was decreased significantly.[15,28,29] The fact that the carrier type changed from p-type to n-type around its stoichiometry in undoped $BaSi_2$ films supported this interpretation.[17] Thus, we conclude that a defect level of V_{Si} located at 0.26 eV below the conduction band minimum (CBM) as a donor level[27 25] and that of Si_i at 0.27 eV above the valence band maximum (VBM)[12] as had been

suggested from the calculation.[16] The P2 is attributed to a transition between Si_i related level and another donor level (0.13 eV)[25] so that its intensity also becomes intense with the increase of Si atomic ratio. Due to the lack of further information on defect levels, the origins of P3 and P4 peaks still remain unclear. However, considering the tendency that both peaks increased under Ba-rich conditions, we speculate that Ba_{Si} is responsible for P3 and P4, and the defect level might be located at approximately 0.1 eV above the VBM. This assumption is considered reasonable because Ba_{Si} induces the defect level above the VBM according to the calculation.[16] Based on the above discussions, we propose a tentative model of radiative defects in $BaSi_2$ as shown in Fig. 5. Please note that the band gap of $BaSi_2$ expands by approximately 0.1 eV at 8 K compared to RT according to the temperature dependence of absorption edge.[30]

In conclusion, we investigated the PL spectra of the *a*-axis-oriented $BaSi_2$ epitaxial films and the polycrystalline $BaSi_2$ bulks. For the films, the increase of growth temperature during MBE growth contributed to the decrease of the nonradiative and/or undetectable defects such as V_{Si}. As a result, the PL intensity was enhanced in the film grown at T_S = 650 °C. From the PL spectra of polycrystalline $BaSi_2$ bulks, we suggest that V_{Si}, Si_i, and Ba_{Si} are assigned to the origins of the PL peaks. A model of PL transitions based on the discussion of the polycrystalline bulks can be applied to those of the films since both the films and the polycrystalline bulks exhibit the same PL peaks.

ACKNOWLEDGEMENTS

This work was financially supported by JSPS KAKENHI Grant Number JP18H03767 and JP16K06713.

Reference

[1] T. Suemasu, Jpn. J. Appl. Phys. **54**, 07JA01 (2015).

[2] T. Suemasu and N. Usami, J. Phys. D: Appl. Phys. **50**, 023001 (2017).

[3] M. Kumar, N. Umezawa, and M. Imai, Appl. Phys. Express **7**, 071203 (2014).

[4] K. Morita, Y. Inomata, and T. Suemasu, Thin Solid Films **508**, 363 (2006).

[5] K. Toh, T. Saito, and T. Suemasu, Jpn. J. Appl. Phys. **50**, 068001 (2011).

[6] M. Baba, K. Toh, K. Toko, N. Saito, N. Yoshizawa, K. Jiptner, T. Sekiguchi, K. O. Hara, N. Usami, and T. Suemasu, J. Cryst. Growth **348**, 75 (2012).

[7] M. Baba, K. Watanabe, K. O. Hara, K. Toko, T. Sekiguchi, N. Usami, and T. Suemasu, Jpn. J. Appl. Phys. **53**, 078004 (2014).

[8] K. O. Hara, N. Usami, K. Toh, M. Baba, K. Toko and T. Suemasu, J. Appl. Phys. **112**, 083108 (2012).

[9] K. O. Hara, N. Usami, K. Nakamura, R. Takabe, M. Baba, K. Toko, and T. Suemasu, Appl. Phys. Express **6**, 112302 (2013).

[10] R. Takabe, K. O. Hara, M. Baba, W. Du, N. Shimada, K. Toko, N. Usami, and T. Suemasu, J. Appl. Phys. **115**, 193510 (2014).

[11] K. Kodama, Y. Yamashita, K. Toko, and T. Suemasu, Appl. Phys. Express **12**, 041005 (2019).

[12] Y. Yamashita, T. Sato, M. E. Bayu, K. Toko and T. Suemasu, Jpn. J. Appl. Phys. **57**, 075801 (2018).

[13] T. Sato, H. Hoshida, R. Takabe, K. Toko, Y. Terai, and T. Suemasu, J. Appl. Phys. **124**, 025301 (2018).

[14] Y. Yamashita, Y. Takahara, T. Sato, K. Toko, A. Uedono, and T. Suemasu, Appl. Phys. Express **12**, 055506 (2019).

[15] T. Sato, C. Lombard, Y. Yamashita, Z. Xu, L. Benincasa, K. Toko, S. Gambarelli, and T. Suemasu, Appl. Phys. Express **12**, 061005 (2019).

[16] M. Kumar, N. Umezawa, W. Zhou, and M. Imai, J. Mater. Chem. A **5**, 25293 (2017).

[17] R. Takabe, T. Deng, K. Kodama, Y. Yamashita, T. Sato, K. Toko, and T. Suemasu, J. Appl. Phys. **123**, 045703 (2018).

[18] M. Tajima, J. Cryst. Growth **103**, 1 (1990).

[19] E. C. Lightowlers, and V. Higgs, Phys. Status Solidi A **138**, 665 (1993).

[20] M. Tajima, Y. Iwata, F. Okayama, H. Toyota, H. Onodera, and T. Sekiguchi, J. Appl. Phys. **111,** 113523 (2012).

[21] S. Kishino, T. Imai, T. Iida, Y. Nakaishi, M. Shinada, Y. Takanashi, and N. Hamada, J. Alloys Compd. **428**, 22 (2007).

[22] L. Benincasa, H. Hoshida, T. Deng, T. Sato, Z. Xu, K. Toko, Y. Terai, and T. Suemasu, J. Phys. Commun. **3**, 075005 (2019).

[23] Y. Inomata, T. Nakamura, T. Suemasu, and F. Hasegawa, Jpn. J. Appl. Phys. **43**, L478 (2004).

[24] M. Baba, M. Kohyama, and T. Suemasu, J. Appl. Phys. **120**, 085311 (2016).

[25] T. Schmidt, K. Lischka, and W. Zulehner, Phys. Rev. B **45**, 8989 (1992).

[26] J. I. Pankove, *Optical processes in semiconductors* (Dover, New York, 1975).

[27] T. Nakamura, T. Suemasu, K. Takakura, F. Hasegawa, A. Wakahara, and M. Imai, Appl. Phys. Lett. **81**, 1032 (2002).

[27] Z. Xu, K. Gotoh, T. Deng, T. Sato, R. Takabe, K. Toko, N. Usami, and T. Suemasu, AIP Advances **8**, 055306 (2018).

[29] Z. Xu, D. A. Shohonov, A. B. Filonov, K. Gotoh, T. Deng, S. Honda, K. Toko, N. Usami, D. B. Migas, V. E. Borisenko, and T. Suemasu, Phys. Rev. Mater. **3**, 065403 (2019).

[30] T. Suemasu, K. Morita, and M. Kobayashi, J. Cryst. Growth **301-302**, 680 (2007).

Fig. 1 (a) PL and (b) PR spectra of samples A (T_S = 580 °C) and B (T_S = 650 °C). The PL spectra were measured at 8 K by a 442 nm laser light with an excitation power of 60 mW/cm^2. The PR spectra were measured at RT under a bias voltage of − 0.5 V applied to the front ITO electrode with respect to the back Al electrode. (c) Raman spectra of samples A and B. The decrease of FWHM of A_g mode indicates that the contribution of V_{Si} deceased in sample B as seen in the inserted figure.

Fig. 2 Temperature dependence of PL spectra of (a) sample C, (b) sample D, (c) sample E, and (d) sample F. (e) A typical fitting result for sample F assuming four Gaussian curves were shown as a red broken line. Each sample contains four different transition as marked by P1, P2, P3, and P4 in the figures.

Fig. 3 (a) PL spectra of polycrystalline bulk samples G-J. Four different transitions were observed at almost the same energies as those observed in the films (Fig. 2). (b) Excitation intensity dependence of PL intensity at 8 K for sample K. All transitions follows $I_{PL} \propto P_{exc}{}^{k}$ (k < 1) as drawn by broken lines.

Fig. 4 Relative PL intensities of (a) the film samples and (b) the polycrystalline bulk samples at 8 K, assuming four Gauss curves.

Fig. 5 Model of radiative defects in $BaSi_2$. Each assignment is discussed in the text.

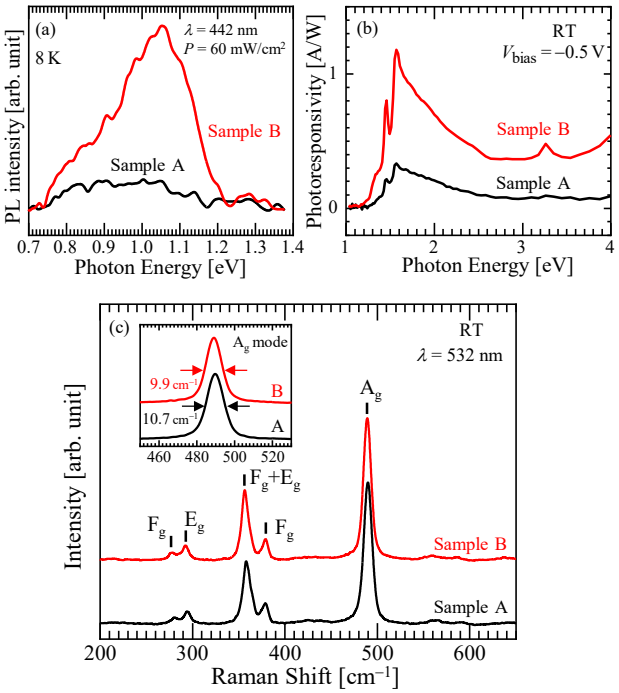
(a)
8 K
λ = 442 nm
P = 60 mW/cm²
Sample B
Sample A
PL intensity [arb. unit]
0.7 0.8 0.9 1.0 1.1 1.2 1.3 1.4
Photon Energy [eV]
(b)
RT
V_bias = −0.5 V
Sample B
Sample A
Photoresponsivity [A/W]
1
0
1 2 3 4
Photon Energy [eV]
(c)
RT
λ = 532 nm
A_g mode
9.9 cm⁻¹
10.7 cm⁻¹
B
A
460 480 500 520
F_g
E_g
F_g
F_g+E_g
A_g
Sample B
Sample A
Intensity [arb. unit]
200 300 400 500 600
Raman Shift [cm⁻¹]

Fig. 1

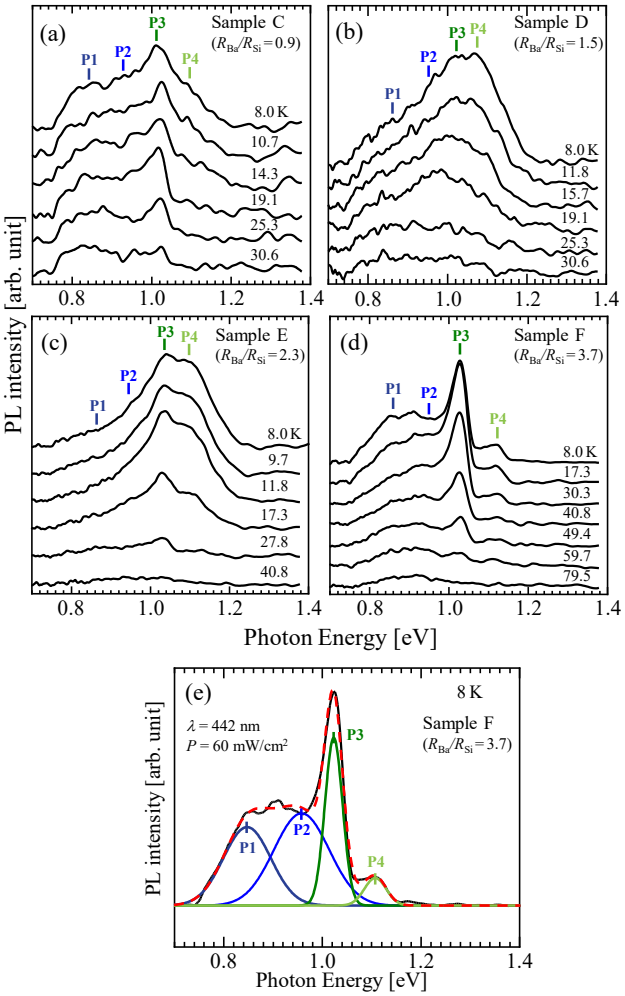
(a)
Sample C
(R_{Ba}/R_{Si} = 0.9)
P1
P2
P3
P4
8.0 K
10.7
14.3
19.1
25.3
30.6
(b)
Sample D
(R_{Ba}/R_{Si} = 1.5)
8.0 K
11.8
15.7
19.1
25.3
30.6
(c)
Sample E
(R_{Ba}/R_{Si} = 2.3)
8.0 K
9.7
11.8
17.3
27.8
40.8
(d)
Sample F
(R_{Ba}/R_{Si} = 3.7)
8.0 K
17.3
30.3
40.8
49.4
59.7
79.5
PL intensity [arb. unit]
Photon Energy [eV]
(e)
8 K
λ = 442 nm
P = 60 mW/cm²
Sample F
(R_{Ba}/R_{Si} = 3.7)
PL intensity [arb. unit]
Photon Energy [eV]

Fig. 2

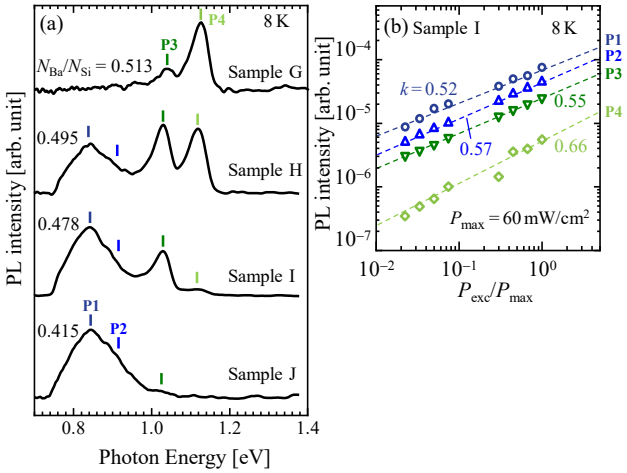
(a)
8 K
P4
P3
N_{Ba}/N_{Si} = 0.513
Sample G
0.495
Sample H
0.478
Sample I
P1
0.415
P2
Sample J
PL intensity [arb. unit]
0.8
1.0
1.2
1.4
Photon Energy [eV]
(b) Sample I
8 K
P1
P2
P3
P4
k = 0.52
0.55
0.57
0.66
P_{max} = 60 mW/cm^2
PL intensity [arb. unit]
10^{-4}
10^{-5}
10^{-6}
10^{-7}
10^{-2}
10^{-1}
10^{0}
P_{exc}/P_{max}

Fig. 3

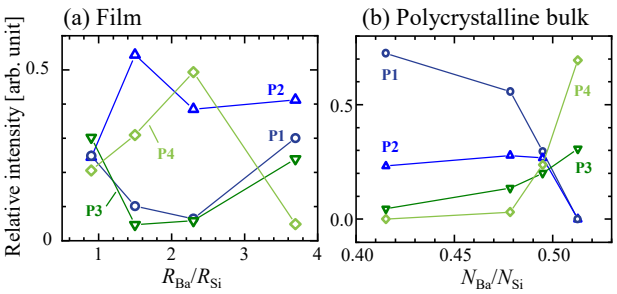
(a) Film
(b) Polycrystalline bulk
Relative intensity [arb. unit]
0.5
0
1
2
3
4
R_{Ba}/R_{Si}
P1
P2
P3
P4
0.5
0.0
0.40
0.45
0.50
N_{Ba}/N_{Si}

Fig. 4

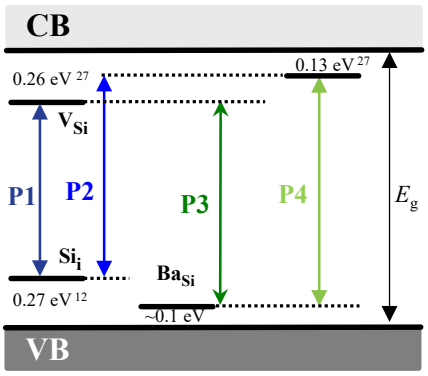

Fig. 5